

Control of modeling errors in the coupling between linear transport and diffusion models

Ludovic Chamoin^a, Laurent Desvillettes^b

^a*LMT-Cachan (ENS Cachan/CNRS/Paris 6 University/PRES UniverSud Paris)
61, Avenue du Président Wilson, 94235 Cachan Cedex*

^b*CMLA (ENS Cachan/CNRS/PRES UniverSud Paris) & IUF
61, Avenue du Président Wilson, 94235 Cachan Cedex*

Abstract

We consider in this paper the initial-boundary value problem for the 1D neutron transport equation with isotropic scattering, set in some bounded interval with entering boundary conditions. The usual parabolic scaling yields the diffusive limit. A surrogate model, coupling transport and diffusion equations, is then introduced in order to accurately assess the value of specific quantities of interest. The control of the quality of the computation (with respect to such a quantity of interest) is performed by means of a modeling error estimation method, coupled to an associated algorithm enabling to adapt the surrogate model if necessary.

Key words: modeling error estimation, adaptive modeling, neutron transport equation, diffusive limit

1. Introduction

The always growing computing resources, associated with more and more precise and validated mathematical models, enable to simulate very complex physical phenomena nowadays. However, there are some families of physical problems for which the initial simulation model is still intractable by current numerical capabilities. A coarser model (usually associated with some homogenization procedure or asymptotic limit, and sometimes involving the coupling of different types of equations) is thus mandatory and leads to a multiscale approach of the problem. For instance, a large set of multiscale methods

Email addresses: chamoin@lmt.ens-cachan.fr (Ludovic Chamoin), laurent.desvillettes@cmla.ens-cachan.fr (Laurent Desvillettes).

has been recently introduced in the context of nano engineering (see [26] for an overview).

In this paper, we deal with physical problems governed by a kinetic equation, and more specifically with problems of neutrons transport (and radiative transfer) which naturally appear in the nuclear industry (or e.g. in astrophysics). The linear kinetic equation which is involved, sometimes referred as linear Boltzmann's equation, takes into account physical phenomena associated with particle transport such as collision, absorption, and emission; its solution enables to know the density of particles with a given velocity at a given space-time coordinate. However, discretization of the transport equation in practical applications involves a huge number of degrees of freedom (since the phase space is of high dimension) which makes a precise simulation a numerical challenge.

When the mean free path of the particles is small w.r.t. the characteristic length of the physical phenomena (that is Knudsen's number Kn is $\ll 1$, cf. [14]), the transport equation can be approximated with a diffusion equation. This latter equation, which can be seen as an homogenized equation at the macroscale, and which concerns the density in the physical space instead of the phase space, is therefore used wherever it is valid, leading to a model reduction and more affordable computations. The resulting coarse model (denoted as the surrogate model in the following) is then made of two coupled concurrent models: (i) a mesoscale model governed by the transport equation and applied in critical subregions where a fine solution is required or in which a macroscale model is not reliable; (ii) a macroscale model governed by the diffusion equation in the rest of the domain.

Usually, the simulation of a physical phenomenon is performed in order to get information on a set of specific quantities of interest. From the analyst's point of view, a critical issue is therefore to know whether or not the simulation model is sufficiently relevant for the assessment of this quantity of interest. In other words, information on modeling and discretization errors is required. During the last decade, and specially in the Computational Mechanics community, tools have been introduced in order to assess the quality of the computerized model [42,43]. Moreover, dedicated algorithms have also been introduced in order to adapt the surrogate model up to an acceptable error level [44,48]. In this paper, we extend these tools to the framework of neutron transport (or radiative transport) simulated with a coupled transport/diffusion model. In order to assess the transferability of these tools to this setting, we consider a simple 1D transport model with isotropic scattering, and choose the neutron macroscopic density at a given point and a given time as the quantity of interest.

The paper is structured as follows: after this introduction, Section 2 describes the reference transport problem; Section 3 presents the surrogate model using the diffusion approximation; in Section 4, we recall basics on modeling error estimation and extend the methodology to the framework of neutrons transport; Section 5 shows some numerical results that illustrate performances of the method; finally, conclusions are drawn in

Section 6.

2. The reference model

2.1. The transport equation

We consider an open bounded domain X of \mathbb{R}^3 , with boundary ∂X , populated with neutrons. Each neutron is defined by its position \mathbf{x} , the direction \mathbf{n} of its velocity, and its velocity modulus v (related to its kinetic energy $E = mv^2/2$). The transport equation [25] describes the evolution of a population of neutrons in this domain occupied by a medium which is in interaction with the neutrons (uranium nuclei for instance). This equation aims at calculating the neutron density in the phase space, denoted by $u(\mathbf{x}, \mathbf{n}, E, t)$, and defined as the probable number of neutrons at position \mathbf{x} with velocity direction \mathbf{n} and energy E at time t .

We also introduce the main macroscopic quantities, that is the neutron density $\rho(\mathbf{x}, E, t)$ of a given energy E , which is the integral of u over all velocity directions:

$$\rho(\mathbf{x}, E, t) := \int_{\Omega} u(\mathbf{x}, \mathbf{n}, E, t) d\mathbf{n}, \quad (1)$$

and the neutron current $\mathbf{j}(\mathbf{x}, E, t)$ of a given energy E :

$$\mathbf{j}(\mathbf{x}, E, t) := \int_{\Omega} v\mathbf{n} u(\mathbf{x}, \mathbf{n}, E, t) d\mathbf{n}, \quad (2)$$

where Ω is the unit sphere of \mathbb{R}^3 .

Denoting by $\Sigma := \Sigma(x)$ the scattering cross section (i.e. the probability of collision per unit distance travelled), and by f the kernel for direction and energy changes of a neutron due to collision, the transport equation satisfied by u reads:

$$\frac{\partial u}{\partial t} + v\mathbf{n} \cdot \nabla_{\mathbf{x}} u + \Sigma v u = \int_{\mathbf{R}_+} \int_{\Omega} \Sigma' f v' u' d\mathbf{n}' dE', \quad \forall (\mathbf{x}, \mathbf{n}, E, t) \in X \times \Omega \times \mathbf{R}_+ \times [0, T] \quad (3)$$

with $u = u(\mathbf{x}, \mathbf{n}, E, t)$, $u' = u(\mathbf{x}, \mathbf{n}', E', t)$, $\Sigma = \Sigma(\mathbf{x}, E)$, $\Sigma' = \Sigma(\mathbf{x}, E')$ and $f = f(\mathbf{x}; \mathbf{n}', E' \rightarrow \mathbf{n}, E)$. Finally, $E' = m|v'|^2/2$. The transport equation thus includes evolution, advection and scattering terms.

Since our objective is to assess the performance of *modeling error control* techniques in the context of kinetic equations, we select one of the simplest meaningful problems: we consider only the elastic scattering occurring within a group of neutrons that all have the same energy E , and we assume that the collision process is isotropic, so that the transport equation consists of finding $u := u(\mathbf{x}, \mathbf{n}, t)$ such that:

$$\frac{\partial u}{\partial t} + v\mathbf{n} \cdot \nabla_{\mathbf{x}} u = \Sigma v \left[\frac{1}{4\pi} \int_{\Omega} u' d\mathbf{n}' - u \right] = -\sigma \mathcal{S}u, \quad \forall (\mathbf{x}, \mathbf{n}, t) \in X \times \Omega \times [0, T] \quad (4)$$

where $u' = u(\mathbf{x}, \mathbf{n}', t)$, $\sigma = \sigma(\mathbf{x}) := \Sigma(\mathbf{x})v$, and \mathcal{S} is the scattering operator.

Note that $\Sigma(\mathbf{x})$ does not need to be bounded below by a strictly positive constant: we keep the possibility that some regions be completely transparent.

In order to scale the problem, we introduce the parameter ε (Knudsen's number) defined as the ratio of the average distance traveled by a neutron between two successive collisions (mean free path $\lambda = 1/\Sigma$) and a characteristic length of the problem. Once the time has also been scaled (in such a way that it is compatible with the typical time of evolution of ρ by diffusion), the transport equation (4) comes down to finding $u_\varepsilon(\mathbf{x}, \mathbf{n}, t)$ such that:

$$\varepsilon \frac{\partial u_\varepsilon}{\partial t} + v\mathbf{n} \cdot \nabla_{\mathbf{x}} u_\varepsilon = -\frac{1}{\varepsilon} \sigma \mathcal{S} u_\varepsilon, \quad \forall (\mathbf{x}, \mathbf{n}, t) \in X \times \Omega \times [0, T]. \quad (5)$$

We impose for the transport problem initial and entering boundary conditions which respectively read:

$$u_\varepsilon(\mathbf{x}, \mathbf{n}, 0) = u_I(\mathbf{x}) \quad \forall (\mathbf{x}, \mathbf{n}) \in X \times \Omega \quad ; \quad u_\varepsilon(\mathbf{x}, \mathbf{n}, t) = u_d(\mathbf{x}, \mathbf{n}, t) \quad \forall (\mathbf{x}, \mathbf{n}) \in \Gamma_- \quad (6)$$

with u_I a given nonnegative function (chosen independent of \mathbf{n} in the paper), and $\Gamma_- = \{(\mathbf{x}, \mathbf{n}) \in \partial X \times \Omega; \boldsymbol{\nu}_{\mathbf{x}} \cdot \mathbf{n} < 0\}$, $\boldsymbol{\nu}_{\mathbf{x}}$ being the outer normal of ∂X at point \mathbf{x} .

2.2. The 1D model

In several cases, equations of transport theory can be written in 1D; this is the case when one considers for X an infinite 2D or 3D strip, of width L on the transversal axis x and invariant by a translation perpendicular to this axis (see [34]). The 1D problem then consists in finding $u_\varepsilon := u_\varepsilon(x, \mu, t)$ such that:

$$\boxed{\begin{aligned} \varepsilon \frac{\partial u_\varepsilon}{\partial t} + \mu v \frac{\partial u_\varepsilon}{\partial x} + \frac{1}{\varepsilon} \sigma \mathcal{S} u_\varepsilon &= 0 \quad \forall (x, \mu, t) \in]0, L[\times]-1, 1[\times [0, T] \\ u_\varepsilon(0, \mu, t) &= u_0(\mu, t), \quad \forall \mu \geq 0 \\ u_\varepsilon(L, \mu, t) &= u_L(\mu, t), \quad \forall \mu \leq 0 \\ u_\varepsilon(x, \mu, 0) &= u_I(x), \end{aligned}} \quad (7)$$

with μ the cosine of the angle between Ox and the velocity (of constant modulus v). For the neutron transport with isotropic scattering we consider, the scattering operator \mathcal{S} then reads:

$$\mathcal{S}u = u - \frac{1}{2} \int_{-1}^1 u(x, \mu', t) d\mu'. \quad (8)$$

In [19], existence and uniqueness of the solution is addressed for problem (7) as well as for the associated stationary problem.

The 1D transport problem (7) can also be written under the weak form:

$$\boxed{\text{Find } u_\varepsilon \in L^\infty \text{ such that } B(u_\varepsilon, w_\varepsilon) = F(w_\varepsilon) \quad \forall w_\varepsilon \in \mathcal{W}} \quad (9)$$

with

$$\begin{aligned} B(u_\varepsilon, w_\varepsilon) &= \int_0^T \int_0^L \int_{-1}^1 u_\varepsilon(x, \mu, t) \left\{ -\varepsilon \partial_t - \mu v \partial_x + \frac{1}{\varepsilon} \sigma \mathcal{S} \right\} w_\varepsilon(x, \mu, t) dx d\mu dt, \\ F(w_\varepsilon) &= \varepsilon \int_{-1}^1 \int_0^L u_I(x) w_\varepsilon(x, \mu, 0) dx d\mu + \int_0^T \int_0^1 \mu w_\varepsilon(0, \mu, t) u_0(\mu, t) d\mu dt \\ &\quad - \int_0^T \int_{-1}^0 \mu w_\varepsilon(L, \mu, t) u_L(\mu, t) d\mu dt, \\ \mathcal{W} &= \{w(x, \mu, t) \in \mathcal{D}([0, L] \times [-1, 1] \times [0, T]); \\ &\quad w(0, \mu, t) = 0 \quad \forall \mu \leq 0, w(L, \mu, t) = 0 \quad \forall \mu \geq 0\}. \end{aligned}$$

\mathcal{D} denotes the space of C^∞ functions with compact support, which implies that functions $w \in \mathcal{W}$ are such that $w(x, \mu, T) = 0$.

2.3. Computation of an approximate solution

Problem (7) can be numerically solved by means of a specific discretization in each dimension. In the present work:

- the space domain $[0, L]$ is divided into P elements, with associated nodes x_p ($p = 1, 2, \dots, P + 1$);
- the time domain $[0, T]$ is divided into N time steps, with associated time points t_n ($n = 1, 2, \dots, N + 1$);
- the velocity domain $[-1, 1]$ is divided into K steps, with associated points μ_k ($k = 1, 2, \dots, K + 1$). In practice, we first divide the angular domain $[-\pi, 0]$ into K angular steps, with angular points θ_k ($k = 1, 2, \dots, K + 1$), and then define $\mu_k = \cos(\theta_k)$.

Using a finite differences algorithm (upwind scheme), the discretized problem reads for $(p, k, n) \in [2, P] \times [1, K + 1] \times [1, N]$:

$$\begin{aligned} \varepsilon \frac{u_\varepsilon^{(p,k,n+1)} - u_\varepsilon^{(p,k,n)}}{\Delta t} + \mu_k v \frac{u_\varepsilon^{(p,k,n)} - u_\varepsilon^{(p-1,k,n)}}{\Delta x} &= \frac{\sigma(x_i)}{\varepsilon} \left(\frac{1}{2} \sum_{k'=1}^{K+1} \alpha_{k'} u_\varepsilon^{(p,k',n)} - u_\varepsilon^{(p,k,n)} \right) \quad \text{if } \mu_k \geq 0 \\ \varepsilon \frac{u_\varepsilon^{(p,k,n+1)} - u_\varepsilon^{(p,k,n)}}{\Delta t} + \mu_k v \frac{u_\varepsilon^{(p+1,k,n)} - u_\varepsilon^{(p,k,n)}}{\Delta x} &= \frac{\sigma(x_i)}{\varepsilon} \left(\frac{1}{2} \sum_{k'=1}^{K+1} \alpha_{k'} u_\varepsilon^{(p,k',n)} - u_\varepsilon^{(p,k,n)} \right) \quad \text{if } \mu_k \leq 0 \\ u_\varepsilon^{(1,k,n)} &= u_0(\mu_k, t_n) \quad \text{if } \mu_k \geq 0 \quad ; \quad u_\varepsilon^{(P+1,k,n)} = u_L(\mu_k, t_n) \quad \text{if } \mu_k \leq 0 \quad ; \quad u_\varepsilon^{(p,k,1)} = u_I(x_p). \end{aligned} \quad (10)$$

Δt and Δx denote time and space steps respectively, whereas coefficients $\alpha_{k'}$ are defined from a numerical integration of the scattering operator (using the trapeze method for instance). Δt and Δx should be chosen so that the Courant-Friedrichs-Lewy (CFL) condition is verified [16,17]. In our 1D case, it reads:

$$\Delta t < \frac{\varepsilon}{v} \Delta x.$$

3. The surrogate model

3.1. Diffusive limit for the transport equation

For media which have a large size compared to the characteristic lengths of the transport equation (mean free path of a neutron), we can obtain an approximate solution of the transport equation by means of a diffusion equation whose coefficients are derived from those of the transport equation. This is the diffusion approximation [25,34], in which the unknown is usually the neutron density ρ . Note that the information about the direction \mathbf{n} of the neutrons velocity is lost in this approximation.

The diffusion approximation is discussed for the neutron transport in [2] and a probabilistic approach of the diffusion approximation is developed in [9]. Besides, in [5], an interpretation of the diffusion approximation is given in terms of an asymptotic behavior of the solution, when time goes to infinity. The physical background for the diffusion approximation is that when the scattering phenomena dominate the streaming effects, the motion of the particles in the medium is almost brownian, and can be modeled by a parabolic equation.

Let us recall that mathematically speaking, one introduces the scaling parameter ε , which leads (in the 1D case) to the scaled system (7). Denoting the neutron density $\rho_\varepsilon(x, t) = \int_{-1}^1 u_\varepsilon(x, \mu, t) d\mu$ and the (rescaled) neutron current $j_\varepsilon(x, t) = \frac{1}{\varepsilon} \int_{-1}^1 \mu v u_\varepsilon(x, \mu, t) d\mu$ (as in (1), (2) but dropping the dependence w.r.t. E), the two following equations can be deduced from (7):

$$\begin{aligned} \frac{\partial \rho_\varepsilon}{\partial t} + \frac{\partial j_\varepsilon}{\partial x} &= 0 && \left(\text{obtained from } \frac{1}{\varepsilon} \int_{-1}^1 \bullet d\mu \right) \\ \varepsilon^2 \frac{\partial j_\varepsilon}{\partial t} + v \frac{\partial}{\partial x} \int_{-1}^1 \mu^2 u_\varepsilon(x, \mu, t) d\mu + \sigma(x) j_\varepsilon &= 0 && \left(\text{obtained from } \int_{-1}^1 \bullet \mu d\mu \right), \end{aligned} \quad (11)$$

where \bullet stands for the 1D transport equation. Combining equations in (11), we get:

$$\frac{\partial \rho_\varepsilon}{\partial t} - \frac{\partial}{\partial x} \left[\frac{1}{\sigma(x)} \left(\varepsilon^2 \frac{\partial j_\varepsilon}{\partial t} + v \frac{\partial}{\partial x} \int_{-1}^1 \mu^2 u_\varepsilon(x, \mu, t) d\mu \right) \right] = 0. \quad (12)$$

When the parameter ε is sufficiently small, the neutron angular density $u_\varepsilon(x, \mu, t)$ (and consequently $\rho_\varepsilon(x, t)$) is correctly approximated by the solution $\hat{u}(x, t)$ of the following

heat equation (see [34,18]):

$$\boxed{\frac{\partial \hat{u}}{\partial t} - \frac{\partial}{\partial x} \left[\frac{2}{3\Sigma(x)} \frac{\partial \hat{u}}{\partial x} \right]} = 0, \quad (13)$$

which can be obtained by assuming that u_ε does not depend on μ when $\varepsilon \rightarrow 0$, and is called the *diffusive limit*. It is associated with the initial condition:

$$\hat{u}(x, 0) = u_I(x) \quad (14)$$

and boundary conditions which are investigated in next section.

Remark 1 In [18] (and [19] in the case of the Fokker-Planck equation), a general diffusive limit for transport equations is given; it reads:

$$\frac{\partial \hat{u}}{\partial t} - \frac{\partial}{\partial x_i} (a_{ij} \frac{\partial \hat{u}}{\partial x_j}) = 0 \quad ; \quad \hat{u}(\mathbf{x}, 0) = u_I(\mathbf{x}) \quad (15)$$

where diffusion coefficients $a_{ij}(\mathbf{x})$, that define a symmetric positive definite matrix, are derived from properties of scattering operator \mathcal{S} .

3.2. Boundary conditions for the diffusion model

3.2.1. Dirichlet boundary conditions

In [18], it is shown that if the boundary conditions for the transport equation are

$$u_\varepsilon(\mathbf{x}, \mathbf{n}, t) = 0, \quad \forall (\mathbf{x}, \mathbf{n}) \in \Gamma_- \quad (16)$$

then the diffusive limit solution \hat{u} , associated with the Dirichlet condition:

$$\hat{u}(\mathbf{x}, t) = 0, \quad \forall \mathbf{x} \in \partial X \quad (17)$$

and initial datum $u_I \in L^\infty$ satisfies:

$$\|u_\varepsilon(\mathbf{x}, \mathbf{n}, t) - \hat{u}(\mathbf{x}, t)\|_{L^\infty(X \times \Omega)} \leq e^{\delta t} C_{u_I} \varepsilon \quad (18)$$

for some $\delta > 0$, where C_{u_I} depends on u_I only. This shows that an order 1 convergence is ensured using Dirichlet boundary conditions for the diffusion model.

3.2.2. Mixed (Robin) boundary conditions

A more accurate, order 2, approximation of the transport model is provided by the use of Robin boundary conditions for the diffusion equation [18]. These mixed boundary conditions take into account the fact that when applying homogeneous Dirichlet boundary conditions (on the microscale transport model), the neutron density actually goes to zero at some distance from the outer boundary of the macroscale diffusion model. The distance d at which it drops off to zero is called the *extrapolation length* [19]; it is related to the mean free path λ by a coefficient Λ ($d = \Lambda\lambda$).

In [18], it is shown that if $u_\varepsilon(\mathbf{x}, \mathbf{n})$ is the solution of the stationary problem:

$$\mathbf{n} \cdot \nabla_{\mathbf{x}} u_\varepsilon + \frac{1}{\varepsilon} \Sigma \mathcal{S} u_\varepsilon = 0 \quad ; \quad u_\varepsilon(\mathbf{x}, \mathbf{n}) = 0 \quad \forall (\mathbf{x}, \mathbf{n}) \in \Gamma_-, \quad (19)$$

and $\hat{u}(\mathbf{x})$ is the solution of (with notations of Remark 1):

$$\frac{\partial}{\partial x_i} (a_{ij} \frac{\partial \hat{u}}{\partial x_j}) = 0 \quad ; \quad \hat{u} + \varepsilon \frac{\Lambda}{\Sigma} \boldsymbol{\nu}_{\mathbf{x}} \cdot \nabla_{\mathbf{x}} \hat{u} = 0 \quad \text{on } \partial X, \quad (20)$$

then for all $p \geq 1$:

$$\|\rho_\varepsilon(\mathbf{x}) - \hat{\rho}(\mathbf{x})\|_{L^p(X)} \leq C_p \varepsilon^2 \quad (21)$$

where C_p depends on p only.

The computation of Λ at point \mathbf{x} on ∂X uses the solution of a conservative Milne problem, which is a stationary problem defined in a semi-infinite domain (cf. [18]). For the 1D transport model we consider, the value of Λ reads:

$$\Lambda = \frac{\sqrt{3}}{2} \int_0^1 \mu^2 H(\mu) d\mu \approx 0,7104 \quad (22)$$

where H is the *Chandrasekhar function* [15].

3.3. Coupling between transport and diffusion models

When simulating transport models, a classical model reduction method consists in replacing the transport equation by the diffusion equation in parts of the domain where this latter equation is relevant. Note that a close problem (but much more complicated) involving the Boltzmann and Navier-Stokes equations was studied in [10,53].

Here, we introduce the diffusive limit model in order to obtain a surrogate model of the transport model, as in [57,58]. We consider the 1D problem (7) of infinite strip with isotropic collision operator. The domain $X =]0, L[$ is divided into two parts $X_t =]0, a[$ and $X_d =]a, L[$ ($0 < a < L$). Assuming that in X_t the diffusion theory gives a poor approximation of the neutron density, the proposed method consists of coupling two models: (i) the transport model used in X_t ; (ii) its diffusion approximation used in X_d .

The coupled problem, with Dirichlet boundary conditions for the diffusion model, thus reads: find the solution pair $(\tilde{u}_\varepsilon, \hat{u})$, where $\tilde{u}_\varepsilon(x, \mu, t)$ (resp. $\hat{u}(x, t)$) is defined in X_t (resp. X_d), such that:

$$\begin{aligned}
& \varepsilon \frac{\partial \tilde{u}_\varepsilon}{\partial t} + \mu v \frac{\partial \tilde{u}_\varepsilon}{\partial x} = -\frac{1}{\varepsilon} \sigma \mathcal{S} \tilde{u}_\varepsilon \quad \text{in } X_t \times [-1, 1] \times [0, T], \\
& \tilde{u}_\varepsilon(x, \mu, 0) = u_I(x) \quad \forall (x, \mu) \in X_t \times [-1, 1], \\
& \tilde{u}_\varepsilon(0, \mu, t) = u_0(\mu, t) \quad \forall \mu \geq 0 \quad ; \quad \tilde{u}_\varepsilon(a, \mu, t) = \hat{u}(a, t) \quad \forall \mu \leq 0; \\
& \frac{\partial \hat{u}}{\partial t} - \frac{\partial}{\partial x} \left(\frac{2}{3\Sigma(x)} \frac{\partial \hat{u}}{\partial x} \right) = 0 \quad \text{in } X_d \times [0, T], \\
& \hat{u}(x, 0) = u_I(x) \quad \forall x \in X_d, \\
& \hat{u}(a, t) = 2 \int_0^1 \tilde{u}_\varepsilon(a, \mu', t) \mu' d\mu' \quad ; \quad \hat{u}(L, t) = 2 \int_{-1}^0 u_L(\mu', t) |\mu'| d\mu'.
\end{aligned} \tag{23}$$

Remark 2 For small mean free paths, the diffusion theory may still fail near the boundary. In this case we only need to take X_t of diameter a few mean free paths away from the boundary; therefore, we need only solve the transport equation in a small domain X_t .

Remark 3 Other couplings could be investigated, such as volume couplings in which the concurrent models overlap (see [8] for instance).

Remark 4 To solve the coupled problem (23) using implicit time schemes, the transmission time marching algorithm can be applied; it considers the following coupling at $x = a$ (for $n \in [1, N]$):

$$\tilde{u}_\varepsilon^{(n+1)}(a, \mu) = \hat{u}^{(n+1)}(a) \quad \forall \mu \leq 0 \quad ; \quad \hat{u}^{(n+1)}(a) = 2 \int_0^1 \tilde{u}_\varepsilon^{(n)}(a, \mu') \mu' d\mu'. \tag{24}$$

It is proved in [58] that this algorithm converges for $0 < a < L$, independently of ε .

Remark 5 When using mixed boundary conditions for the diffusion model, the following conditions should be considered:

$$\begin{aligned}
\hat{u}(a, t) - \frac{\Lambda(a)\varepsilon}{\Sigma(a)} \frac{\partial \hat{u}}{\partial x}(a, t) &= 2 \int_0^1 \tilde{u}_\varepsilon(a, \mu', t) \mu' d\mu' \\
\hat{u}(L, t) + \frac{\Lambda(L)\varepsilon}{\Sigma(L)} \frac{\partial \hat{u}}{\partial x}(L, t) &= 2 \int_{-1}^0 u_L(\mu', t) |\mu'| d\mu'
\end{aligned} \tag{25}$$

which results in the new relation in the transmission time marching algorithm:

$$\hat{u}^{(n+1)}(a) - \frac{\Lambda(a)\varepsilon}{\Sigma(a)} \frac{\partial \hat{u}^{(n+1)}}{\partial x}(a) = 2 \int_0^1 \tilde{u}_\varepsilon^{(n)}(a, \mu') \mu' d\mu'. \tag{26}$$

The model coupling transport and diffusion equations is denoted as the surrogate model in the following. It can be written under the weak form:

$$\text{find } (\tilde{u}_\varepsilon, \hat{u}) \in L^\infty \text{ such that } B_0((\tilde{u}_\varepsilon, \hat{u}), (\tilde{w}_\varepsilon, \hat{w})) = F_0(\tilde{w}_\varepsilon, \hat{w}) \quad \forall (\tilde{w}_\varepsilon, \hat{w}) \in \mathcal{W}_c, \tag{27}$$

where

$$\begin{aligned}
\mathcal{W}_c &= \{(\tilde{w}, \hat{w}) \in \mathcal{D}([0, L] \times [-1, 1] \times [0, T]) \times \mathcal{D}([0, L] \times [0, T]) \\
&\quad \text{s.t. } \hat{w}(a, t) = \hat{w}(L, t) = 0, \\
&\quad \tilde{w}(0, \mu, t) = 0 \quad \text{when } \mu \leq 0, \\
&\quad \tilde{w}(a, \mu, t) = 0 \quad \text{when } \mu \geq 0\}, \\
B_0((\tilde{u}_\varepsilon, \hat{u}), (\tilde{w}_\varepsilon, \hat{w})) &= \int_0^T \int_{X_t} \int_{-1}^1 \tilde{u}_\varepsilon(x, \mu, t) \left\{ -\varepsilon \partial_t - \mu v \partial_x + \frac{1}{\varepsilon} \sigma S \right\} \tilde{w}_\varepsilon(x, \mu, t) dx d\mu dt \\
&\quad + \int_0^T \int_{X_d} \hat{u}(x, t) \left\{ -\partial_t \hat{w} - \partial_x \left(\frac{3}{2\Sigma(x)} \partial_x \hat{w} \right) \right\} (x, t) dx dt \\
&\quad + \int_0^T \frac{3}{2\Sigma(a)} \partial_x \hat{w}(a, t) 2 \int_0^1 \tilde{u}_\varepsilon(a, \mu', t) \mu' d\mu' dt \\
&\quad + \int_0^T \int_{-1}^0 \mu \tilde{w}_\varepsilon(a, \mu, t) \hat{u}(a, t) d\mu dt, \\
F_0(\tilde{w}_\varepsilon, \hat{w}) &= \int_{-1}^1 \int_{X_t} u_I(x) \tilde{w}_\varepsilon(x, \mu, 0) dx d\mu + \int_{X_d} u_I(x) \hat{w}(x, 0) dx \\
&\quad + \int_0^T \int_0^1 \mu \tilde{w}_\varepsilon(0, \mu, t) u_0(\mu, t) d\mu dt \\
&\quad + \int_0^T \frac{3}{2\Sigma(L)} \partial_x \hat{w}(L, t) 2 \int_{-1}^0 u_L(\mu', t) |\mu'| d\mu' dt
\end{aligned} \tag{28}$$

if Dirichlet boundary conditions \mathcal{C}_D are applied to the diffusion model.

4. Modeling error estimation and model adaptation

In this section, we introduce the methodology used to assess discretization and modeling errors that occur in numerical simulations. In our case, it will specifically be used to control the quality of the surrogate model that couples transport and diffusion equations. The error estimates and adaptive control procedures that it enables to derive are targeted to specific quantities of interest and are thus referred to as *goal-oriented*. The development of such numerical tools has been the object of numerous works in recent years [42,43,47,4,48].

4.1. Definition of the error on a quantity of interest

We recall that the reference 1D transport problem (cf. (9)) reads:

$$\boxed{\text{Find } u_\varepsilon \in L^\infty \text{ such that } B(u_\varepsilon, w_\varepsilon) = F(w_\varepsilon) \quad \forall w_\varepsilon \in \mathcal{W}.} \tag{29}$$

We are interested in a specific feature of the solution u_ε , i.e. a linear quantity of interest denoted $Q(u_\varepsilon)$. The functional Q can be written under the generic form:

$$Q(u_\varepsilon) = \int_0^T \int_{-1}^1 \int_0^L g(x, \mu, t) u_\varepsilon(x, \mu, t) dx d\mu dt, \quad (30)$$

where g is a distribution called the *extraction function* or *extractor*.

In practical cases, the reference problem is intractable and we are led to consider a coupled problem (cf. (27)) that reads:

$$\boxed{\text{Find } u_0 \in \mathcal{U}_0 \subset L^\infty \text{ such that } B_0(u_0, w_0) = F_0(w_0) \quad \forall w_0 \in \mathcal{W}_0 \subset \mathcal{W}} \quad (31)$$

with $u_0(x, \mu, t) = \tilde{u}_\varepsilon(x, \mu, t)$ in X_t and $u_0(x, \mu, t) = \hat{u}(x, t)$ in X_d .

The modeling error in the quantity of interest Q that we aim to assess thus reads:

$$\mathcal{E}_{mod} = Q(u_\varepsilon) - Q(u_0). \quad (32)$$

Remark 6 In practice, the numerical simulations enable to compute an approximate solution u_0^h of u_0 only; we can thus define the total error on Q :

$$\mathcal{E} = Q(u_\varepsilon) - Q(u_0^h) = [Q(u_\varepsilon) - Q(u_0)] + [Q(u_0) - Q(u_0^h)] = \mathcal{E}_{mod} + \mathcal{E}_{dis} \quad (33)$$

where \mathcal{E}_{mod} (resp. \mathcal{E}_{dis}) is the error on Q due to modeling (resp. due to discretization).

4.2. Adjoint problem and goal-oriented error estimation

In [6], an optimal control approach is proposed in order to deal with errors on Q ; it is based on a constrained minimization framework and leads to an adjoint problem of the form:

$$\boxed{\text{Find } p_\varepsilon \in \mathcal{W} \text{ such that } B'(u_\varepsilon; w_\varepsilon, p_\varepsilon) = Q'(u_\varepsilon; w_\varepsilon) \quad \forall w_\varepsilon \in \mathcal{W},} \quad (34)$$

where B' and Q' are Gâteaux-derivatives of B and Q , respectively. The solution p_ε , seen as an influence function, depends on the quantity of interest. In our case, B and Q are respectively bilinear and linear functionals so that the adjoint problem reduces to:

$$\boxed{\text{Find } p_\varepsilon \in \mathcal{W} \text{ such that } B(w_\varepsilon, p_\varepsilon) = Q(w_\varepsilon) \quad \forall w_\varepsilon \in \mathcal{W}.} \quad (35)$$

Remark 7 Physically speaking, adjoint problem (35) is a transport problem similar to (7), except that it is reverse in time (with zero final conditions), has homogeneous entering boundary conditions, and is loaded by a source term represented by the extractor g . It reads in its strong form:

$$\begin{aligned} \left(-\varepsilon \frac{\partial p_\varepsilon}{\partial t} - \mu v \frac{\partial p_\varepsilon}{\partial x} + \frac{1}{\varepsilon} \sigma \mathcal{S} p_\varepsilon \right) (x, \mu, t) &= g(x, \mu, t) \quad \forall (x, \mu, t) \in]0, L[\times [-1, 1] \times [0, T], \\ p_\varepsilon(0, \mu, t) &= 0 \quad \forall \mu \leq 0 \quad ; \quad p_\varepsilon(L, \mu, t) = 0 \quad \forall \mu \geq 0 \quad ; \quad p_\varepsilon(x, \mu, T) = 0 \end{aligned} \quad (36)$$

and can be discretized in a way similar to (10).

Remark 8 When considering a quantity of interest in a time domain prior to $t_0 < T$, the adjoint problem needs to be solved on $[0, t_0]$ only (the adjoint solution for $t > t_0$ is zero).

Again, the adjoint problem is usually not tractable and needs to be replaced by a coupled problem of the form:

$$\boxed{\text{Find } p_0 \in \bar{\mathcal{W}}_0 \text{ such that } \bar{B}_0(w_0, p_0) = Q(w_0) \quad \forall w_0 \in \bar{\mathcal{W}}_0} \quad (37)$$

where \bar{B}_0 and $\bar{\mathcal{V}}_0$ are similar to B_0 and \mathcal{V}_0 except that domain X_t in which the transport model is conserved is taken a bit larger. In practice, the interface between the concurrent coupled models is placed at $x = \bar{a} := a + \Delta a$, with $\Delta a > 0$.

We can now define the following residual functionals, associated with reference and adjoint problems respectively:

$$\begin{aligned} \mathcal{R}(u_0, w) &:= F(w) - B(u_0, w) \quad \forall w \in \mathcal{W}, \\ \bar{\mathcal{R}}(p_0, w) &:= Q(w) - B(w, p_0) \quad \forall w \in \mathcal{W}. \end{aligned} \quad (38)$$

They represent the degree to which u_0 and p_0 fail to satisfy the reference and adjoint problems (29) and (35).

In [43], a general relation is established between the modeling error in the quantity of interest and the residual functionals. In our case, it merely reads:

$$\mathcal{E}_{mod} = Q(u_\varepsilon) - Q(u_0) = \mathcal{R}(u_0, p_\varepsilon) = \mathcal{R}(u_0, p_0) + \mathcal{R}(u_0, \varepsilon_0), \quad (39)$$

where $\varepsilon_0 = p_\varepsilon - p_0$ is the error on the adjoint solution. Assuming that this error is small, a good estimate of the modeling error on the quantity of interest is:

$$\mathcal{E}_{mod} \approx \mathcal{R}(u_0, p_0). \quad (40)$$

Remark 9 A more accurate error estimate would consist in assessing ε_0 using a global error estimate; however, this procedure is problem-dependent and more costly.

Remark 10 When taking discretization error \mathcal{E}_{dis} into account, other estimates can be set up:

- First, an estimate of the total error on the quantity of interest reads:

$$\mathcal{E} \approx \mathcal{R}(u_0^h, p_0^h), \quad (41)$$

where u_0^h and p_0^h are computed solutions obtained after discretizations of coupled reference and adjoint problems.

- Second, if one wants to assess the discretization error only, a good estimate is:

$$\mathcal{E}_{dis} \approx \mathcal{R}_0(u_0^h, p_0^h) := F_0(p_0^h) - B_0(u_0^h, p_0^h), \quad (42)$$

i.e. an estimate defined taking the coupled problem (31) as the reference.

Let us notice that only estimates (41) and (42) are actually computable. Therefore, a relevant error estimation process consists in first assessing the discretization error \mathcal{E}_{dis} and checking that it is small in order to use the estimate $\mathcal{E}_{mod} \approx \mathcal{E} \approx \mathcal{R}(u_0^h, p_0^h)$.

4.3. Goal-oriented model adaptation

When using a surrogate model, such as the one presented in the previous section and based on a coupling between transport and diffusion models, it is fundamental to be able to adapt this surrogate model if need be. In our case, assuming that the discretization error can be neglected, the adaptation of the surrogate model consists in enlarging the region X_t in which the transport model lies, up to obtaining a sufficiently accurate value for the quantity Q .

Therefore, we come up with an adaptive greedy algorithm that aims at controlling the modeling error \mathcal{E}_{mod} within some preset error tolerance γ_{tol} . This is generally achieved by generating a sequence of surrogate problems with solutions (u_0^k, p_0^k) so that for some integer k_0 , the modeling error satisfies:

$$\left| Q(u_\varepsilon) - Q(u_0^{k_0}) \right| \leq \gamma_{tol}. \quad (43)$$

At each iteration, the goal is to reduce the global quantity $\mathcal{R}(u_0, p_0)$ by locally enriching the surrogate model, i.e. by locally switching on the transport model in the subregions where the diffusion model is not accurate enough. This is possible by observing that the residual term $\mathcal{R}(u_0, p_0)$ is defined globally over the whole domain and can be decomposed into local contributions η_c defined over predefined subdomains (generally finite elements of the mesh used to discretize the diffusion model in space). Finally, prescribing a user-defined parameter γ_a such that $0 < \gamma_a < 1$, the subdomains with contributions η_c can be switched from the diffusion model to the transport model whenever $\eta_c > \gamma_a \max_c \eta_c$.

The proposed greedy algorithm for adaptation of the surrogate model, denoted *Goals Algorithm*, reads as follows:

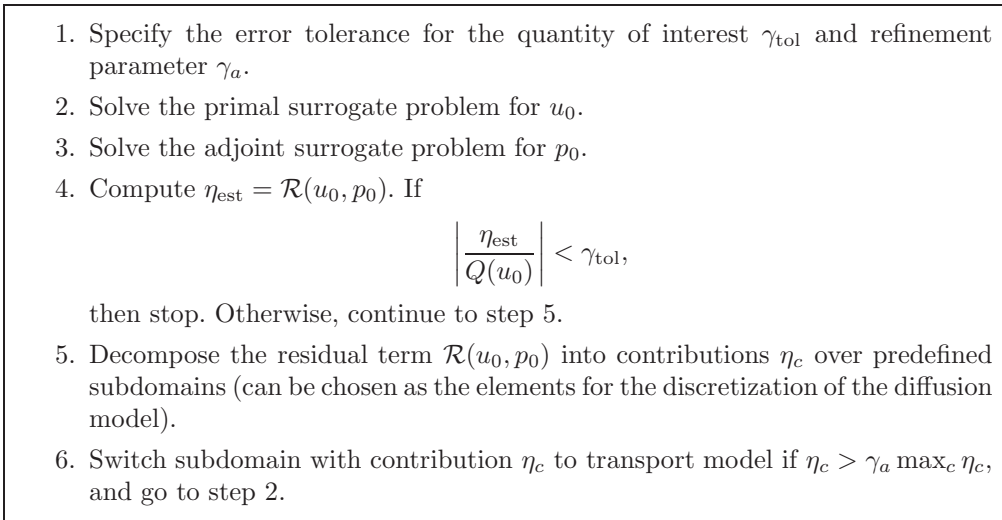


Figure 1. Greedy algorithm for goal-oriented error estimation and control of modeling error.

Remark 11 An optimized adaptive approach would consist in splitting the estimate $\mathcal{R}(u_0, p_0)$ into contributions over each finite element and each time step, so that the coupled model can be adapted both in space and time. However, this procedure is technically more complex to set up.

5. Numerical results

In all the following numerical experiments, we consider 1D transport problems with constant velocity modulus $v = 1$ and isotropic scattering, defined over a time-space domain $]0, L[\times]0, T[$ with $L = 5$ and $T = 4$. We take zero initial conditions ($u_I(x) = 0$) and prescribe for all $t \in [0, T]$ the following entering boundary conditions:

$$u_0(\mu, t) = 1 \quad \forall \mu \geq 0 \quad ; \quad u_L(\mu, t) = 0 \quad \forall \mu \leq 0. \quad (44)$$

Scaling parameter is fixed to $\varepsilon = 5 \cdot 10^{-2}$, and we consider a piecewise linear evolution for $\Sigma(x)$ (see Fig.2):

- $\Sigma(x) = \varepsilon$ for $x \in [0, 2]$;
- $\Sigma(x)$ evolves linearly from ε to 1 for $x \in [2, 3]$;
- $\Sigma(x) = 1$ for $x \in [3, 5]$.

Therefore, $\Sigma/\varepsilon = 1$ in the transparent part of the domain, and we intend that the diffusion model is valid in the left-hand side of the domain.

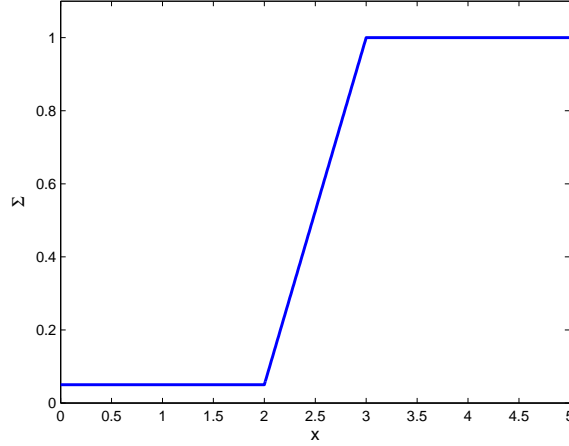


Figure 2. Evolution of the scattering cross section Σ over the space domain.

The discretizations of transport and diffusion models are performed the following way:

- for the transport model ($x \in X_t$), we use the finite differences scheme defined in (10);
- for the diffusion model ($x \in X_d$), we use a classical finite elements method associated with a forward Euler scheme in time.

Even though, in practical applications, larger time steps Δt and space steps Δx should be used for the discretization of the diffusion model, we use here the same values as for the discretization of the transport model. For this last model, the CFL condition reads ($v = 1$):

$$\Delta t < \varepsilon \Delta x. \quad (45)$$

Furthermore, in order to represent the scattering phenomenon correctly, the time step should verify:

$$\Delta t \ll \frac{\varepsilon^2}{\sigma} \quad (46)$$

and as regards the diffusion model, the stability condition reads:

$$\Delta t < \frac{\Sigma \Delta x^2}{2}. \quad (47)$$

In the following, we thus choose $\Delta x = 0.1$ and $\Delta t = 10^{-5}$.

For the neutron transport problem we study, interesting quantities of interest may be the neutron density ρ_ε or the neutron flux j_ε ; we thus consider these two quantities of interest at a given space-time point $(x_Q, t_Q) \in]0, L[\times]0, T[$:

$$Q_1(u_\varepsilon) = \int_{-1}^1 u_\varepsilon(x_Q, \mu, t_Q) d\mu \quad ; \quad Q_2(u_\varepsilon) = \frac{1}{\varepsilon} \int_{-1}^1 \mu u_\varepsilon(x_Q, \mu, t_Q) d\mu, \quad (48)$$

which leads to extractors $g_1(x, \mu, t) = \delta_{x_Q}(x)\delta_{t_Q}(t)$ and $g_2(x, \mu, t) = \frac{\mu}{\varepsilon}\delta_{x_Q}(x)\delta_{t_Q}(t)$, respectively. The Dirac loading which is involved is in practice approximated with a pointwise force $f = 1/(\Delta t \Delta x)$ located at node n_Q and time t_Q . In the following, we take $x_Q = 1.5$ and $t_Q = 3.8$.

5.1. Results with the linearized Carleman model

For practical reasons regarding clarity of the parametric studies and understanding of the displayed results by the reader, we first apply the error estimation methodology to a simplified one-dimensional model of (7), denoted as the linearized Carleman model [51]. This model, in which $\mu = \pm 1$, simulates the collision between two neutron populations evolving in inverse directions. The associated phase space densities are denoted $u^+(x, t)$ and $u^-(x, t)$, respectively. The scaled problem, which describes a random walk in 1D, consists of finding $u_\varepsilon^+(x, t)$ and $u_\varepsilon^-(x, t)$ such that:

$$\begin{aligned} \varepsilon \frac{\partial u_\varepsilon^+}{\partial t} + \frac{\partial u_\varepsilon^+}{\partial x} &= \frac{\sigma(x)}{2\varepsilon}(u_\varepsilon^- - u_\varepsilon^+) \quad ; \quad \varepsilon \frac{\partial u_\varepsilon^-}{\partial t} - \frac{\partial u_\varepsilon^-}{\partial x} = \frac{\sigma(x)}{2\varepsilon}(u_\varepsilon^+ - u_\varepsilon^-) \\ u_\varepsilon^+(0, t) &= u_0(t) \quad ; \quad u_\varepsilon^-(L, t) = u_L(t) \quad ; \quad u_\varepsilon^\pm(x, 0) = u_I(x) \end{aligned} \quad (49)$$

This system, also known as the Goldstein-Taylor model [29], can be reduced to a damped wave equation i.e. the telegrapher's equation [39].

5.1.1. Exact and approximate solutions

We represent in Fig. 3 the (quasi-)exact solution of problem (49), computed with an overkill discretization, in the space-time domain; in practice, this solution would be unknown. The associated values (taken as reference) of the quantities of interest are $Q_1 = 1.8398$ and $Q_2 = 1.2814$.

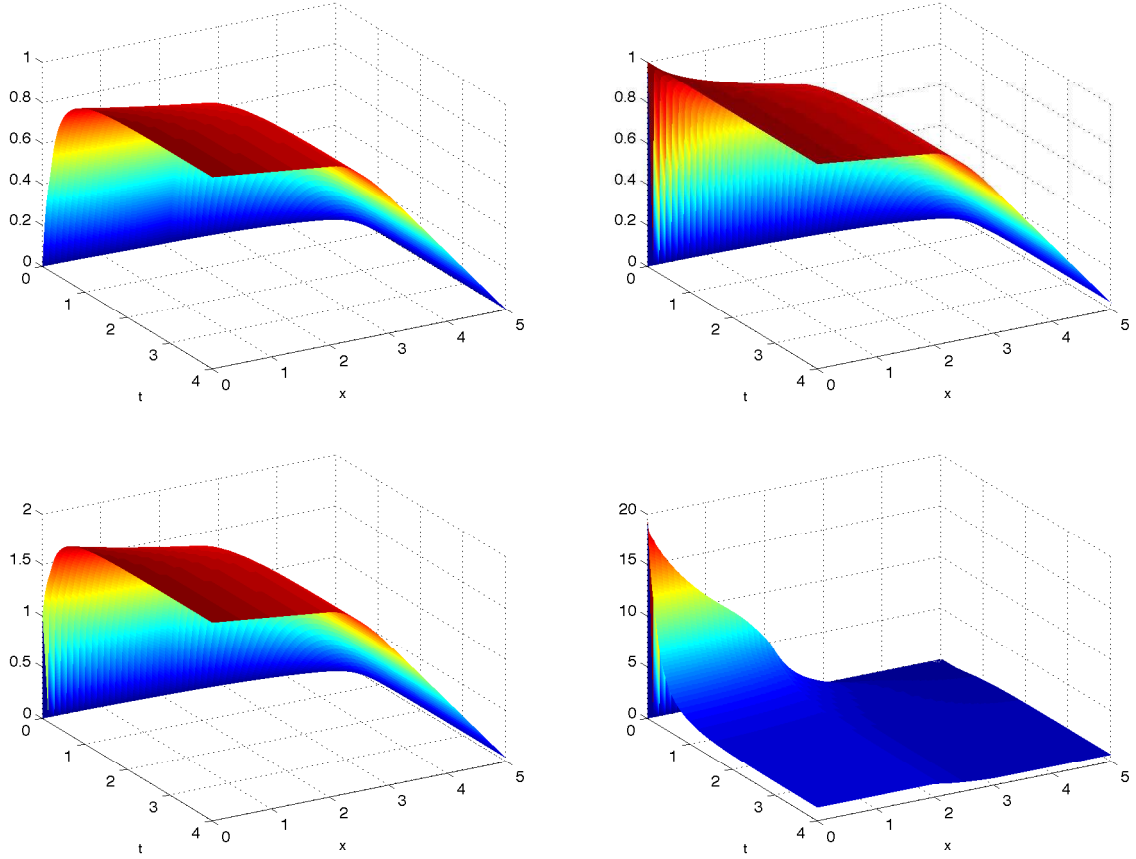


Figure 3. Exact solution of the linearized Carleman model in the space-time domain: u_ε^- (top left), u_ε^+ (top right), ρ_ε (bottom left), j_ε (bottom right).

The diffusive limit for the linearized Carleman model reads:

$$\frac{\partial \hat{u}}{\partial t} - \frac{\partial}{\partial x} \left[\frac{1}{\Sigma(x)} \frac{\partial \hat{u}}{\partial x} \right] = 0. \quad (50)$$

In this diffusive limit, the neutron current j_ε is of order ε , so that we can use the approximation $u_\varepsilon^+ = u_\varepsilon^- = \rho_\varepsilon/2$. Furthermore, the extrapolation length Λ is here equal to 1.

We show in Fig. 4 the approximate solution (density and flux) obtained with the transport-diffusion coupled model, with three different positions $a \in [0, L]$ of the interface i.e. $a = 1.0$, $a = 2.0$ and $a = 3.0$. We use mixed boundary conditions for the diffusion model here.

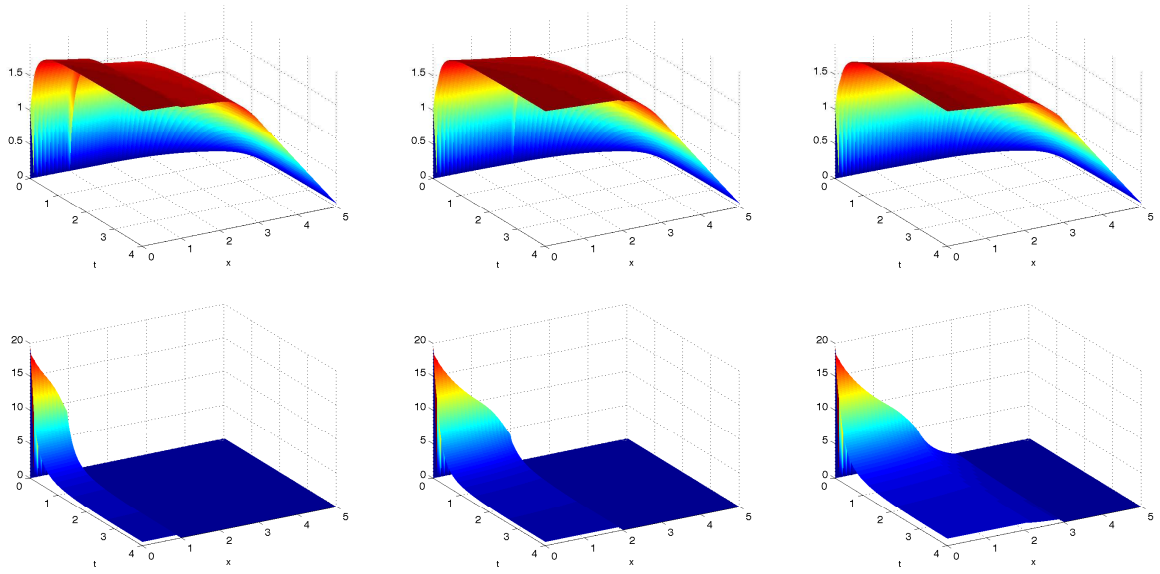


Figure 4. Approximate solution of the linearized Carleman model in the space-time domain, for $a = 1$ (left), $a = 2.0$ (center), $a = 3.0$ (right): density ρ_0 (top), flux j_0 (bottom).

We clearly observe that the solution is corrupted when the interface is placed in (or close) to the transparent zone. The associated approximate values of quantities of interest Q_1 and Q_2 are given in Tab. 1.

a	Q_1	error on Q_1 (%)	Q_2	error on Q_2 (%)
1.0	1.8967	3.09	0.0000	100.00
2.0	1.9295	4.88	0.5621	56.13
3.0	1.8693	1.60	1.0435	18.57

Table 1

Values of Q_1 and Q_2 with respect to the position of the interface between transport and diffusion models.

5.1.2. Error estimation

We now use the error estimation strategy introduced in Section 4 in order to adapt the model up to a given level. We give in Fig. 5 (resp. Fig. 6) the approximate solutions (density and flux) of the adjoint problems associated to Q_1 (resp. Q_2), for an interface placed at $\tilde{a} = 2.5$.

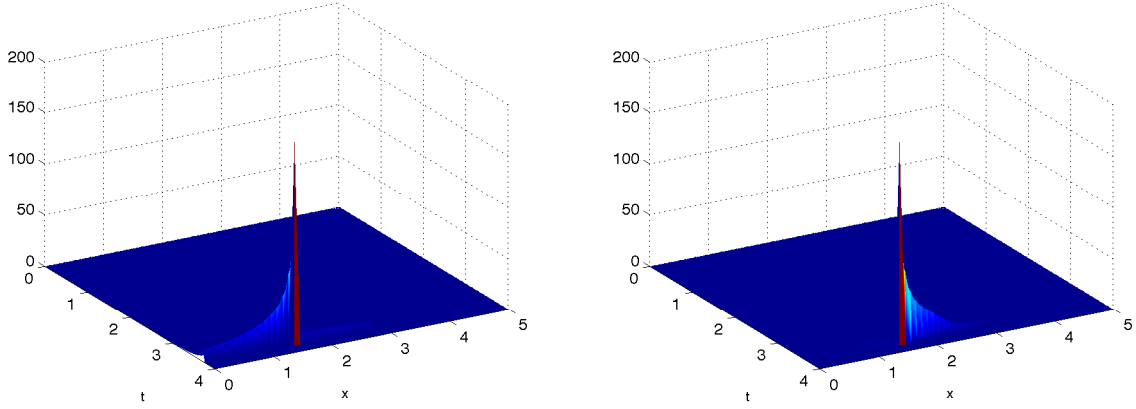


Figure 5. Approximate adjoint solution, in the space-time domain, for $Q_1: p_0^-$ (left), p_0^+ (right).

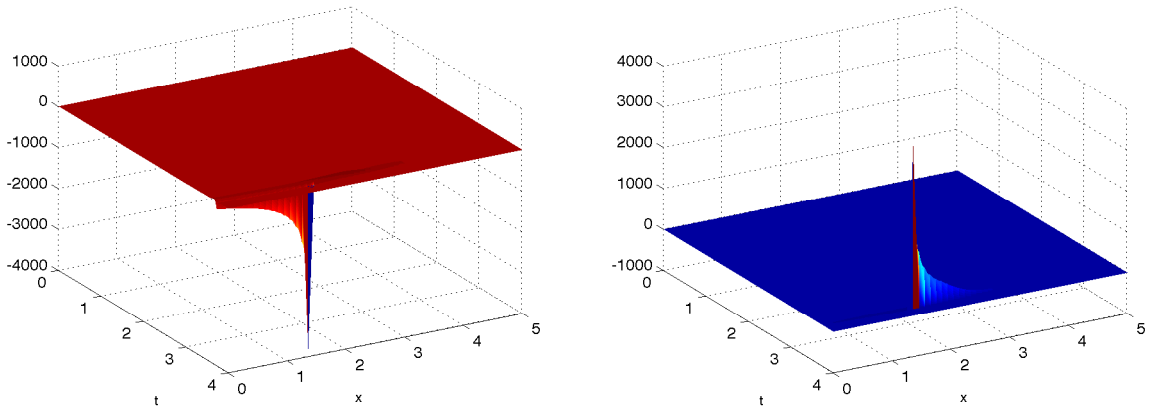


Figure 6. Approximate adjoint solution, in the space-time domain, for $Q_2: p_0^-$ (left), p_0^+ (right).

We observe that these solutions are very localized in space and time, and have high gradient near the coordinates where quantities of interest are computed.

Before computing a modeling error estimate, we check that the discretization error remains neglectable. In the case $a = 2.0$, we compute for Q_1 the discretization error estimate defined in Section 4.2. The representation of this estimate in the space-time domain is shown in Fig.7. We observe that the discretization error is concentrated in the area of point (x_Q, t_Q) , and extends a little bit around that point.

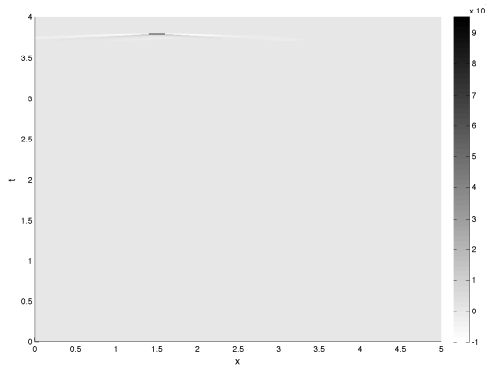


Figure 7. Contributions in space and time to the discretization error for Q_1 .

The value of the relative global discretization error estimate for Q_1 is 0.61%, which is small compared to the total error on Q_1 (4.88%) given in Tab. 1. This confirms that the discretization we consider is accurate enough to address the issue of modeling error.

Still considering an approximate solution with $a = 2.0$, we now compute the estimate $\mathcal{R}(u_0, p_0)$ associated to Q_1 for various positions \tilde{a} of the interface in the adjoint coupling problem. Results are reported In Tab. 2.

\tilde{a}	2.0	2.2	2.4	2.6	2.8	3.0
estimate (%)	1.27	4.29	4.87	5.03	5.03	5.03

Table 2

Values of error estimate for Q_1 , with respect to the position \tilde{a} of the adjoint interface.

We observe that the estimate converges very rapidly, and that extending the transport domain, for the coupled adjoint problem, beyond $\tilde{a} = 2.6$ does not change the value of the estimate. Therefore, in all the following computations, we will consider $\tilde{a} = a + 0.5$.

5.1.3. Model adaptation

We now use the *Goals algorithm* presented in Section 4.3 in order to drive the goal-oriented model adaptation with respect to Q_1 or Q_2 . In both cases, we start from an initial position $a = 1.6$ for the interface, and specify error tolerance $\gamma_{tol} = 3\%$ and refinement parameter $\gamma_a = 0.2$. To illustrate the adaptation process, we plot in Fig. 8 contributions of residual $\mathcal{R}(u_0, p_0)$, associated to Q_1 and for $a = 2$, over each subdomain in the physical space.

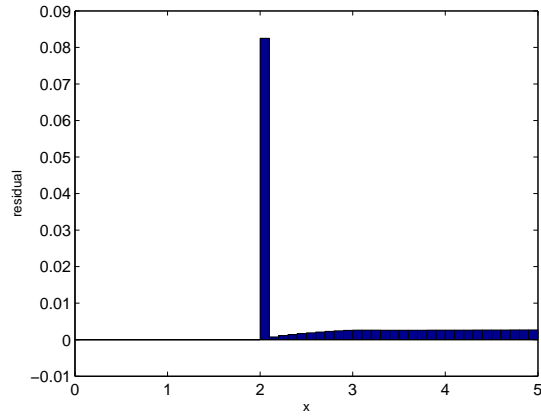


Figure 8. Spatial contributions of the residual for $a = 2$.

We give in Tab. 3 (resp. Tab. 4) the obtained approximate values of Q_1 (resp. Q_2) along iterations of the adaptive algorithm, considering either Dirichlet or mixed boundary conditions for the diffusion model.

Dirichlet BC				Mixed BC			
iteration #	a	Q_1	estimate (%)	iteration #	a	Q_1	estimate (%)
0	1.6	2.0827	15.25	0	1.6	1.9767	7.69
1	1.9	1.9701	7.34	1	1.8	1.9426	5.81
2	2.2	1.9366	5.43	2	2.0	1.9295	4.99
3	2.4	1.9011	3.49	3	2.1	1.8877	2.73
4	2.5	1.8934	2.91				

Table 3
Values of a , Q_1 , and error estimate on Q_1 for each iteration of the Goals algorithm.

Dirichlet BC				Mixed BC			
iteration #	a	Q_2	estimate (%)	iteration #	a	Q_2	estimate (%)
0	1.6	0.3239	80.01	0	1.6	0.2734	80.81
1	1.9	0.4957	64.88	1	2.0	0.5621	59.11
2	2.3	0.6860	49.13	2	2.4	0.7311	43.29
3	2.7	0.8791	33.40	3	2.9	1.0396	19.86
4	3.3	1.0844	16.09	4	3.2	1.1794	8.22
5	3.5	1.1797	8.29	5	3.5	1.2319	4.19
6	3.6	1.1923	7.17	6	3.6	1.2492	2.91
7	3.7	1.2104	5.74				
8	3.8	1.2232	4.81				
9	4.0	1.2516	2.66				

Table 4

Values of a , Q_2 , and error estimate on Q_2 for each iteration of the Goals algorithm.

5.2. Results with 1D neutron transport problem

We consider now the reference model presented in Section 2.2. We represent in Fig. 9 the (quasi-)exact solution of this problem, computed with an overkill discretization, in the space-time domain. The associated values (taken as reference) of the quantities of interest are $Q_1 = 1.7997$ and $Q_2 = 0.6020$.

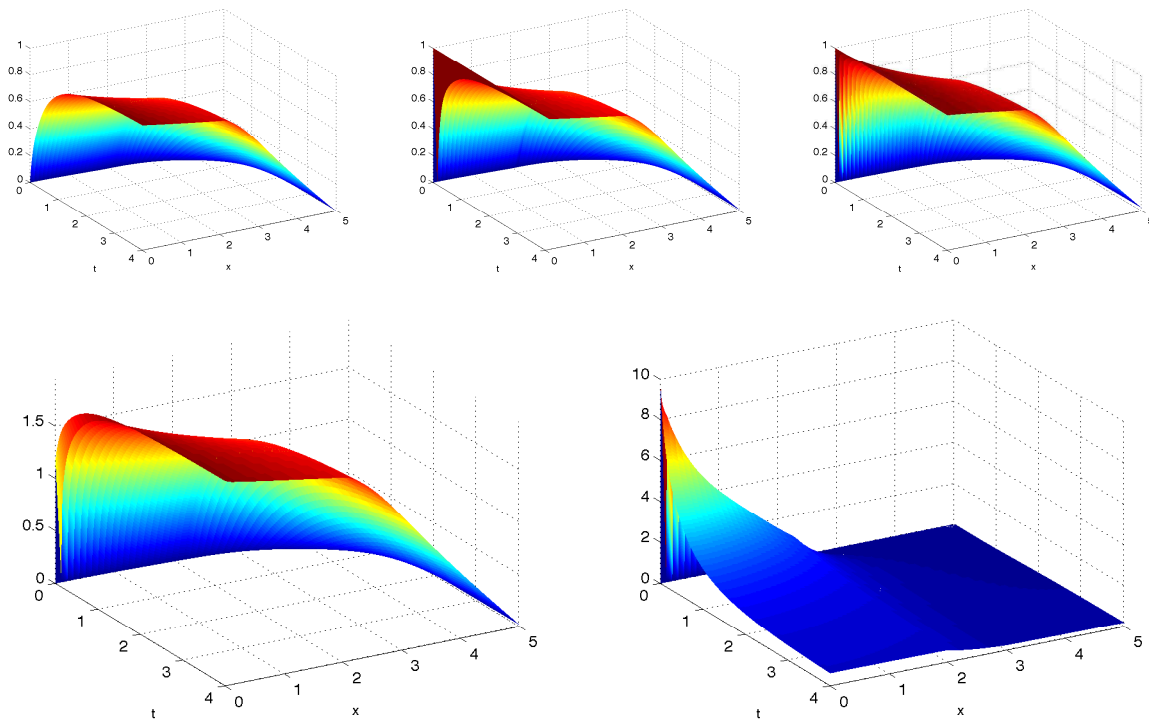


Figure 9. Exact solution of 1D neutron transport model in the space-time domain: neutron density in the phase space u_ε (top) for $\mu = -1$, $\mu = 0$, and $\mu = 1$ (from left to right), density ρ_ε (bottom left), flux j_ε (bottom right).

Starting again from an initial position $a = 1.6$ for the interface, and specifying error tolerance $\gamma_{tol} = 3\%$ and refinement parameter $\gamma_a = 0.2$, we perform the modeling adaptation. We give in Tab. 5 (resp. Tab. 6) the obtained approximate values of Q_1 (resp. Q_2) along iterations of the adaptive algorithm, considering either Dirichlet or mixed boundary conditions for the diffusion model.

Dirichlet BC				Mixed BC			
iteration #	a	Q_1	estimate (%)	iteration #	a	Q_1	estimate (%)
0	1.6	2.1244	20.04	0	1.6	2.0329	13.77
1	1.8	2.0133	12.66	1	1.8	1.9502	10.06
2	2.0	1.9124	7.02	2	1.9	1.8663	4.12
3	2.1	1.8377	2.51	3	2.0	1.8111	1.22

Table 5
Values of a , Q_1 , and error estimate on Q_1 for each iteration of the Goals algorithm.

Dirichlet BC				Mixed BC			
iteration #	a	Q_2	estimate (%)	iteration #	a	Q_2	estimate (%)
0	1.6	0.2044	68.61	0	1.6	0.3626	42.40
1	2.0	0.4678	24.19	1	1.8	0.5711	6.49
2	2.2	0.5432	10.54	2	2.1	0.5799	4.28
3	2.4	0.5571	7.98	3	2.2	0.5859	3.04
4	2.6	0.5709	5.77	4	2.3	0.5905	2.42
5	2.7	0.5823	3.99	5			
6	2.8	0.5888	2.71	6			

Table 6

Values of a , Q_2 , and error estimate on Q_2 for each iteration of the Goals algorithm.

5.3. Results with the generalized Carleman model

Finally, we apply our method for modeling error estimation and model adaptation to the nonlinear generalized Carleman model. This model, that takes saturation effects into account, involves a collision frequency that is proportional to some power of the macroscopic density $\rho_\varepsilon = u_\varepsilon^+ + u_\varepsilon^-$. It reads (for $v = 1$):

$$\begin{aligned} \varepsilon \frac{\partial u_\varepsilon^+}{\partial t} + \frac{\partial u_\varepsilon^+}{\partial x} &= \frac{1}{\varepsilon} \rho_\varepsilon^\alpha (u_\varepsilon^- - u_\varepsilon^+) \quad ; \quad \varepsilon \frac{\partial u_\varepsilon^-}{\partial t} - \frac{\partial u_\varepsilon^-}{\partial x} = \frac{1}{\varepsilon} \rho_\varepsilon^\alpha (u_\varepsilon^+ - u_\varepsilon^-) \\ u_\varepsilon^+(0, t) &= u_0(t) \quad ; \quad u_\varepsilon^-(L, t) = u_L(t) \quad ; \quad u_\varepsilon^\pm(x, 0) = u_I(x) \end{aligned} \quad (51)$$

System (51) has been studied by several authors using variety of analytical techniques [32,52,38,31]. Assuming sufficient regularity on the initial data u_I , uniqueness of the solution has been addressed in [37].

in [30], it was shown that the diffusive limit for the generalized Carleman model is governed by the nonlinear diffusion equation:

$$\partial_t \hat{\rho} = \frac{1}{2} \partial_{xx} \left(\frac{\hat{\rho}^{1-\alpha}}{1-\alpha} \right) = \frac{1}{2} \partial_x \left(\frac{1}{\hat{\rho}^\alpha} \partial_x \hat{\rho} \right) \quad (52)$$

for $\alpha \in [-1, 1[$, while the case $\alpha = 1$ leads to $\partial_t \hat{\rho} = \frac{1}{2} \partial_{xx} \ln \hat{\rho}$. This diffusive limit can be viewed as the Navier-Stokes equation of a fictitious gas.

Remark 12 The justification of the limit process for different choices of α has been addressed in [37,49,50]. It was particularly shown that the solution $\hat{\rho}$ is not unique in the range $\alpha \in [1, 2]$. In that case, the limit is the unique maximal solution which conserves the mass.

In the following, we take $\alpha = 0.5$. We represent in Fig. 10 the (quasi-)exact solution of problem (51) computed with an overkill discretization. The associated values (taken as reference) of the quantities of interest are $Q_1 = 0.9789$ and $Q_2 = 0.5692$.

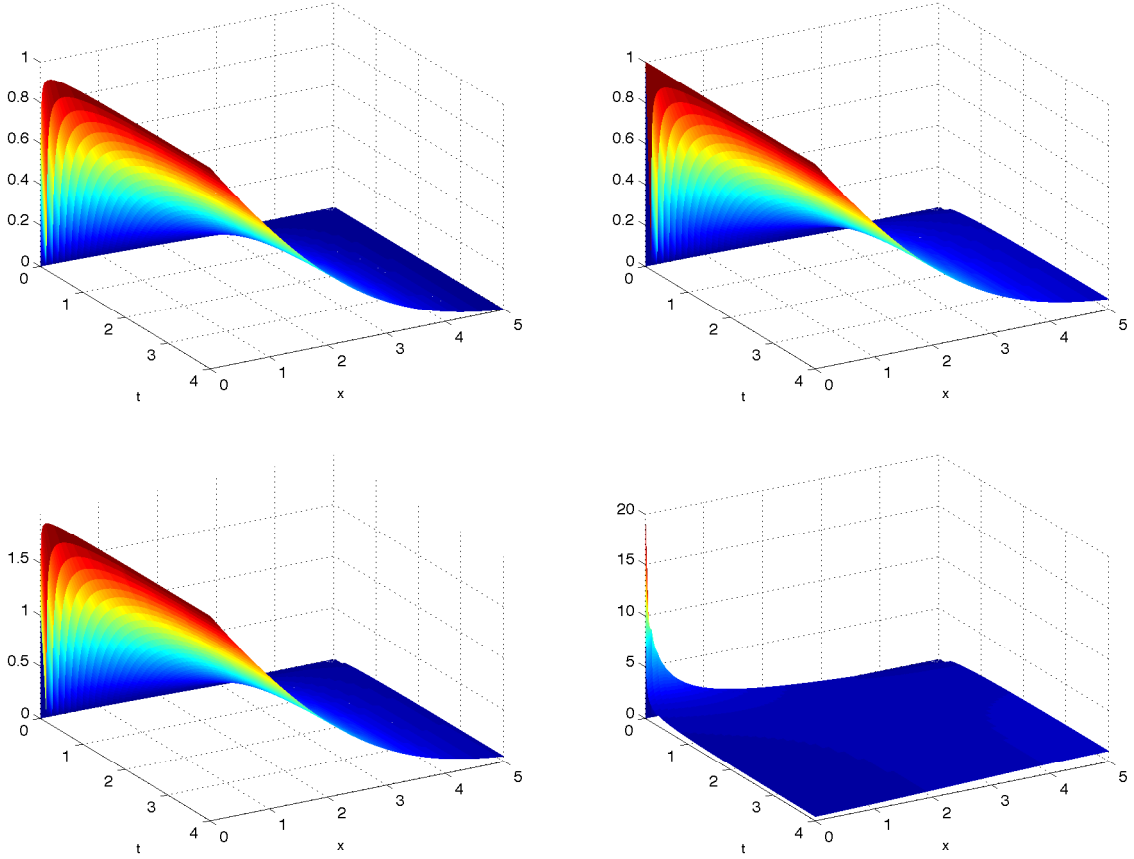


Figure 10. Exact solution of the generalized Carleman model in the space-time domain: u_ε^- (top left), u_ε^+ (top right), ρ_ε (bottom left), j_ε (bottom right).

We then solve the surrogate model obtained by coupling transport and diffusion models, and we perform the modeling adaptation using the same parameters as in previous sections. Let us notice that the adjoint problem considers here linearized (tangent) operators of the generalized Carleman model. We give in Tab. 7 (resp. Tab. 8) the obtained approximate values of Q_1 (resp. Q_2) along iterations of the adaptive algorithm, considering either Dirichlet or mixed boundary conditions for the diffusion model.

Dirichlet BC				Mixed BC			
iteration #	a	Q_1	estimate (%)	iteration #	a	Q_1	estimate (%)
0	1.6	1.2113	25.72	0	1.6	1.1349	17.12
1	1.8	1.0901	12.80	1	1.8	1.0490	8.68
2	2.0	1.0655	9.39	2	2.0	0.9935	2.16
3	2.2	1.0323	6.36				
4	2.3	1.0021	2.88				

Table 7
Values of a , Q_1 , and error estimate on Q_1 for each iteration of the Goals algorithm.

Dirichlet BC				Mixed BC			
iteration #	a	Q_2	estimate (%)	iteration #	a	Q_2	estimate (%)
0	1.6	0.3612	38.79	0	1.6	0.4799	18.33
1	1.8	0.4398	24.29	1	1.7	0.5180	10.17
2	2.1	0.4821	16.33	2	1.9	0.5347	7.70
3	2.3	0.5211	9.72	3	2.1	0.5496	4.06
4	2.5	0.5427	5.81	4	2.2	0.5560	2.61
5	2.7	0.5538	2.98				

Table 8
Values of a , Q_2 , and error estimate on Q_2 for each iteration of the Goals algorithm.

6. Conclusion

We developed a framework for goal-oriented error estimation and model adaptation when neutron transport models are solved by means of surrogate models. These last models, in which the fine transport model is replaced with a coarse diffusion model in some part of a physical domain, are therefore controlled in order to provide the value of given quantities of interest with prescribed accuracy. The procedure uses the solution of an adjoint problem as well as a specific algorithm that drives the adaptive process by moving the interface between concurrent models accordingly. Numerical experiments on 1D transport models showed performances of the approach and its capabilities to provide for an optimal surrogate model (in terms of accuracy and computational cost).

In forthcoming works, the technique will be applied to 2D and 3D transport models, in which speed directions on Ω are fully considered. As the transport problem is multi-parametric, reduction methods based on separation of variables can be very effective; it thus will be useful to test the error estimation and modeling adaptation strategy in such cases.

References

- [1] Babuška I, Strouboulis T. *The finite element method and its reliability*. Oxford university press, 2001.
- [2] Bardos C, Santos R, Sentis R. Diffusion approximation and computation of the critical size. *Transactions of the American Mathematical Society* 1984; **284**.
- [3] Bardos C, Golse F, Perthame B, Sentis R. The nonaccretive radiative transfer equations: existence of solutions and Rosseland approximation. *J. Funct. Anal.* 1988; **77**(2):434–460.
- [4] Bauman P.T, Oden J.T, Prudhomme S. Adaptive multiscale modeling of polymeric materials: Arlequin coupling and goals algorithms. *Computer Methods in Applied Mechanics and Engineering* 2009; **198**:799–818.
- [5] Beals R, Protopopescu V. On the asymptotic equivalence of the Fokker-Planck and diffusion equations. *Transport Theory and Statistical Physics* 1983; **12**(2):109–127.
- [6] Becker R, Rannacher R. An optimal control approach to a posteriori error estimation in finite element methods. *Acta Numerica* 2001; **10**:1–102.
- [7] Bellouquid A. Limite asymptotique pour le modèle de Carleman. *Comptes Rendus Académie des Sciences, Maths, Paris* 1995; **321**(5):655–658.
- [8] Ben Dhia H, Rateau G. The Arlequin method as a flexible engineering design tool. *International Journal for Numerical Methods in Engineering* 2005; **62**(11):1442–1462.
- [9] Bensoussan A, Lions J.L, Papanicolaou G.C. Boundary layers and homogenization of transport processes. *J. Publ. RIMS Kyoto Univ.* 1979; **15**:53–157.
- [10] Bourgat J.F, Le Tallec P, Tidriri M.D. Coupling Navier-Stokes and Boltzmann. *J. Comp. Phys.* 1996; **127**:227–245.
- [11] Bourgade J.P. *Obtention de modèles de diffusion à partir d'équations cinétiques: modélisation, étude mathématique et simulation*. PhD Thesis, 2004.
- [12] Carleman T. *Problèmes mathématiques dans la théorie cinétique des gaz*. Almqvist-Wiksell, Uppsala, 1957.
- [13] Cartier J. *Résolution de l'équation du transport par une méthode éléments finis mixtes-hybrides et approximation par la diffusion de problèmes de transport*. PhD Thesis, 2006.
- [14] Cercignani C. *The Boltzmann Equation and its Applications*. Springer-Verlag, New-York, 1988.
- [15] Chandrasekhar S. *Radiative Transfer*. Oxford university press, London, 1950.
- [16] Courant R, Friedrichs K, Lewy H. Über die partiellen differenzgleichungen der mathematischen physik. *Mathematische Annalen* 1928; **100**(1):32–74.
- [17] Courant R, Friedrichs K, Lewy H. On the partial difference equations of mathematical physics (English translation of the 1928 German original). *IBM Journal* 1967; 215–234.
- [18] Dautray R, Lions J-L. *Analyse Mathématique et Calcul Numérique pour les Sciences et les Techniques*. Masson, 1987.
- [19] Degond P, Mas-Gallic S. Existence of solutions and diffusion approximation for a model Fokker-Planck equation. *Transport Theory and Statistical Physics* 1987; **16**(4-6):589–636.
- [20] Degond P, Zhang K. Diffusion approximation of a scattering matrix model of a semiconductor superlattice. *SIAM J. Appl. Math.* 2002; **63**(1):279–298.
- [21] Densmore J.D, Urbatsch T.J, Evans T.M, Buksas M.W. A hybrid transport-diffusion method for Monte-Carlo radiative transfer simulations. *J. Computational Phys.* 2007; **222**:485–503.
- [22] Desvillettes L, Graham C, Méléard S. Probabilistic interpretation and numerical approximation of a Kac equation without cutoff. *Stochastic Processes and Applications* 1999; **84**(1):115–135.
- [23] Desvillettes L, Lin C. Non local thermodynamical equilibrium line radiative transfer: quasi-stationary approximation. *Proceedings of WASCOP 2007–14th Conference on Waves and Stability in Continuous Media, World Sci. Publ., Singapore* 2008; 218–27.
- [24] Desvillettes L, Salvarani F. Asymptotic behavior of degenerate linear transport equations. *Bulletin des Sciences Mathématiques* 2009; **133**(8):848–858.

- [25] Duderstadt J.J, Martin W.R. *Transport Theory*. Wiley, New York, 1979.
- [26] Fish J. Bridging the scales in nano engineering and science. *Journal of Nanoparticle Research* 2006; **8**(6):577–594.
- [27] Fitzgibbon W.E. Initial boundary value problems for the Carleman equation. *Comp. & Maths with Appls* 1983; **9**(3):519–525.
- [28] Godillon-Lafitte P, Goudon T. A coupled model for radiative transfer: Doppler effects, equilibrium, and nonequilibrium diffusion asymptotics. *Multiscale Model. Simul.* 2005; **4**(4):1245–1279.
- [29] Goldstein S. On diffusion by discontinuous movements, and on the telegraph equation. *Quart. J. Mech. Appl. Math.* 1951; **4**:129–156.
- [30] Golse F, Salvarani F. The nonlinear diffusion limit for generalized Carleman models: the initial-boundary value problem. *Nonlinearity* 2007; **20**:927–942.
- [31] Kaper H, Leaf G. Initial value problems for the Carleman equation. *J. Nonlinear Analysis* 1980; **4**:343–362.
- [32] Koledner I. On Carleman’s model for the Boltzman equation and its generalizations. *Ann. Mat. Pura Appl. Ser. 4* 1963; **63**:11–32.
- [33] Ladevèze P, Pelle J-P. *Mastering Calculations in Linear and Nonlinear Mechanics*. Springer NY, 2004.
- [34] Larsen E, Keller J.B. Asymptotic solutions of neutron transport problems. *J. Math. Phys.* 1974; **15**:75–81.
- [35] Latocha V. *Deux problèmes en transport des particules chargées intervenant dans la modélisation d’un propulseur ionique*. PhD Thesis, 2001.
- [36] Le Tallec P, Tidriri M.D. Application of maximum principles to the analysis of a coupling time marching algorithm. *J. Math. Anal. Appl.* 1999; **229**:158–169.
- [37] Lions P.L, Toscani G. Diffusive limits for finite velocities Boltzmann kinetic models. *Rev. Mat. Iberoamericana* 1997; **13**:473–513.
- [38] Martin R.H. *Nonlinear Operators and Differential Equations in Banach Spaces*. Wiley, New York, 1976.
- [39] McKean H.P. The central limit theorem for Carleman’s equation. *Israel J. Math.* 1975; **21**:54–92.
- [40] Mihalas D, Mihalas B. *Foundations of radiation hydrodynamics*. Oxford University Press, New York, 1984.
- [41] Oden J.T, Zohdi T.I. Analysis and adaptive modeling of highly heterogeneous elastic structures. *Computer Methods in Applied Mechanics and Engineering* 1997; **148**:367.
- [42] Oden J.T, Vemaganti K. Estimation of local modeling error and goal-oriented modeling of heterogeneous materials. Part I: Error estimates and adaptive algorithms. *Journal of Computational Physics* 2000; **164**:22–47.
- [43] Oden J.T, Prudhomme S. Estimation of modeling error in computational mechanics. *Journal of Computational Physics* 2002; **182**:496–515.
- [44] Oden J.T, Babuška I, Nobile F, Feng Y, Tempone R. Theory and methodology for estimation and control of error due to modeling, approximation, and uncertainty. *Computer Methods in Applied Mechanics and Engineering* 2005; **194**:195–204.
- [45] Paraschivoiu M, Peraire J, Patera A.T. A posteriori finite element bounds for linear functional outputs of elliptic partial differential equations. *Computer Methods in Applied Mechanics and Engineering* 1997; **150**:289–312.
- [46] Pomraning G.C, Foglesong C.M. Transport-diffusion interfaces in radiative transfer. *J. Computational Phys.* 1979; **32**:420–436.
- [47] Prudhomme S, Bauman P.T, Oden J.T. Error control for molecular statics problems. *International Journal for Multiscale Computational Engineering* 2006; **4**:647–662.
- [48] Prudhomme S, Chamoin L, Ben Dhia H, Bauman P.T. An adaptive strategy for the control of modeling error in two-dimensional atomic-to-continuum coupling simulations. *Computer Methods in Applied Mechanics and Engineering* 2009; **198**(21-26):1887–1901.
- [49] Salvarani F, Vasquez J.L. The diffusive limit for Carleman-type equations. *Nonlinearity* 2005; **18**:1223–1248.

- [50] Salvarani F, Toscani G. The diffusive limit of Carleman-type models in the range of very fast diffusion equations. *Journal of Evolution Equations* 2009; **9**:67–80.
- [51] Taylor G.I. Diffusion by continuous movements. *Proc. London Math. Soc.* 1922; **20**:196–212.
- [52] Teman R. Sur la résolution exacte et approchée d'un problème hyperbolique non linéaire de T. Carleman. *Arch. Rat. Mech. Anal.* 1969; **35**:351–362.
- [53] Tidriri M.D. *Couplage d'approximations et de modèles de types différents dans le calcul d'écoulements externes*. PhD Thesis, 1992.
- [54] Tidriri M.D. Numerical analysis of coupling for a kinetic equation. *Mathematical Modelling and Numerical Analysis* 1999; **33**(6):1121–1134.
- [55] Tidriri M.D. Asymptotic analysis of a coupled system of kinetic equations. *Comptes Rendus Académie des Sciences, Paris* 1999; **328**:637–642.
- [56] Tidriri M.D. Asymptotic analysis of the coupling of transport equations and their diffusion approximations. *Comptes Rendus Académie des Sciences, Paris* 2000; **330**:1073–1078.
- [57] Tidriri M.D. An alternative model to boundary layers correctors in transport theory and radiative transfer. *Comptes Rendus Académie des Sciences, Paris* 2001; **333**:195–200.
- [58] Tidriri M.D. New models for the solution of intermediate regimes in transport theory and radiative transfer: existence theory, positivity, asymptotic analysis, and approximations. *Journal of Statistical Physics* 2001; **104**(1-2):291–325.